Thermochimica Acta, 236 (1994) 93–104
Elsevier Science B.V., Amsterdam
SSDI 0040-6031(93)01547-G

Mutual influences between ammonium heptamolybdate and γ-alumina during their thermal treatments

A.A. Said

Chemistry Department, Faculty of Science, Assiut University, Assiut, Egypt

(Received 7 July 1993; accepted 30 July 1993)

Abstract

Different proportions of ammonium heptamolybdate (AHM) supported on γ-alumina were prepared by the impregnation method. The thermal decomposition stages of AHM and the solid products were investigated using DTA, TG, XRD and IR techniques. The results obtained revealed that the absence of all peaks accompanying the decomposition stages of AHM at low loading levels (<20 mol%) was due to the dispersion capacity of the support. On increasing the % loading of AHM, γ-alumina retarded the formation of the two intermediates, $(NH_4)_4Mo_7O_{23} \cdot 2H_2O$ and $(NH_4)_2Mo_7O_{22} \cdot 2H_2O$, while favoring the decomposition of the latter to produce solid MoO_3. The produced MoO_3 readily interacted with Al_2O_3 above 500°C to form $Al_2(MoO_4)_3$ phase which became highly crystallized when calcined at 700°C. The aluminum molybdate spinel formed was thermally stable up to 800°C, and then decomposed above this temperature into α-Al_2O_3 and MoO_3. Moreover, the Al_2O_3 support decreased the crystallinity of MoO_3, whereas $Al_2(MoO_4)_3$ only affected the surface-active site, Mo=O. Finally, the presence of MoO_3 greatly enhanced the crystallization of alumina into the κ- and α-phases upon heating at 700 and 900°C, respectively.

INTRODUCTION

In recent years, alumina-supported catalysts have attracted considerable interest because of the increasing number and variety of their industrial and technological applications. Many of these materials have been described as so-called monolayer catalysts [1]. These catalysts are typically prepared by impregnation of the support oxide with an appropriate salt from aqueous solution. Under certain conditions, the materials formed by impregnation can undergo solid-state reactions during thermal treatment in which cations of the active component may be incorporated into the support oxide matrix. Stable surface compounds may thus be formed, for example surface spinels [2, 3]. Molybdenum oxides supported on alumina are one of the most important classes of solid catalysts [4]. An overwhelming problem related to supported metal oxide catalysts is the establishment of a close relation between the catalytic activity and the physicochemical properties of the active phase [5–8]. It has been reported that heating a mixture of ammonium heptamolybdate and γ-alumina leads to the formation of highly

crystalline MoO_3 or $Al_2(MoO_4)_3$ compounds [9, 10]. Many studies have been concerned with the structure of these catalysts and it appears that the choice of the support and its loading are the most important factors. Thus, the mutual effects between Al_2O_3 support and ammonium heptamolybdate during their thermal treatments still need further investigation. Therefore, the present work was devoted to the study of the thermal decomposition of ammonium heptamolybdate in the presence of γ-alumina support, as well as to the identification of the compounds resulting from the solid–solid interaction between MoO_3 and Al_2O_3. The techniques employed were TG, DTA, X-ray diffraction and IR spectroscopy.

EXPERIMENTAL

Materials

The starting materials were Analar grade chemicals. γ-Alumina, prepared by precalcination of $Al(OH)_3$ in air at 500°C, was impregnated with different proportions of ammonium heptamolybdate (AHM), $(NH_4)_6Mo_7O_{24} \cdot 4H_2O$, dissolved in bidistilled water. The samples were dried in an oven at 100°C to constant weight. The proportions of AHM ranged between 5 and 40 mol%. The parent mixture solids were calcined at 400, 550, 700 and 900°C for 5 h.

Techniques

Thermogravimetry (TG) and differential thermal analysis (DTA) of pure AHM and the various impregnated solids were carried out using a Shimadzu computerized thermal analysis system DT-40. The system includes programs which process data from the thermal analyzer with the chromatopac C-R3A. The rate of heating of samples was kept at 10°C min^{-1} using dry air atmosphere flowing at 40 cm^3 min^{-1}. α-Alumina was used as a DTA reference standard.

X-ray diffractometry (XRD) of the thermal products of pure AHM and of AHM supported on γ-alumina was performed with a Phillips diffractometer (PW 1010), with a Cu target and Ni filter. The diffraction patterns were matched with ASTM cards [11].

Infrared spectra (IR) of the thermal products of pure AHM and of AHM supported on γ-alumina were recorded from KBr discs using a Pye Unicam SP 3-300 spectrophotometer.

RESULTS AND DISCUSSION

Thermal decomposition of pure AHM and of AHM supported on γ-alumina

TG and DTA curves of pure AHM and of AHM supported on γ-alumina are shown in Fig. 1. The DTA curve of pure AHM, $(NH_4)_6Mo_7O_{24} \cdot 4H_2O$,

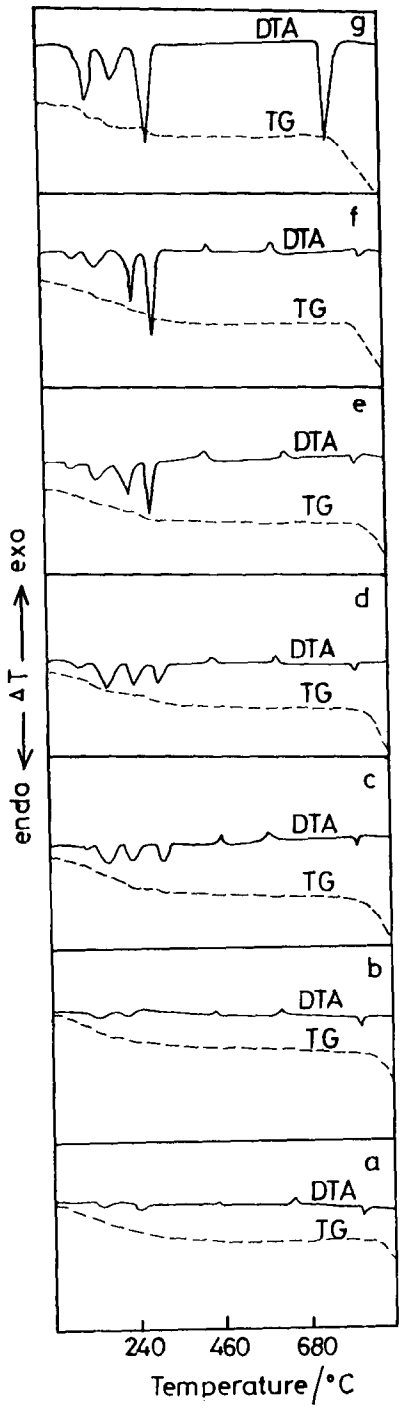

Fig. 1. TG and DTA curves of pure AHM (g) and of AHM supported on γ-Al_2O_3, loading: 15 mol% (a), 20 mol% (b), 25 mol% (c), 30 mol% (d), 35 mol% (e), and 40 mol% (f).

(curve g) exhibits four endothermic peaks at 124, 202, 300 and 780°C, respectively. The TG curve shows that AHM looses weight in four stages on heating up to 900°C. The first peak was followed by about 7.2% mass loss corresponding to the evolution of three H_2O and two NH_3 molecules and formation of the intermediate $(NH_4)_4Mo_7O_{23} \cdot 2H_2O$. The second peak, associated with 4.2% mass loss, corresponded to the elimination of one H_2O and two NH_3 molecules, and formation of the second intermediate $(NH_4)_2Mo_7O_{22} \cdot 2H_2O$. The third, sharp, strong peak was accompanied by 6.9% weight loss due to the decomposition of the second intermediate to MoO_3, with elimination of three H_2O and two NH_3 molecules [12]. The formation of MoO_3 shows subsequent notable thermal stability up to 750°C. The last, sharp, strong peak centered at 780°C related to the melting of MoO_3 [13]; this was followed by sublimation and complete weight loss. In fact, pure MoO_3 undergoes sublimation upon heating at temperatures above its melting point (795°C) [14].

The results of the DTA and TG curves of AHM supported on γ-alumina, Fig. 1, curves a–f, can be summarized as follows.

(i) The DTA curves of the samples containing low ratios of AHM (<15 mol%) on γ-alumina did not show any peaks corresponding to the decomposition of AHM, whereas the TG curves indicated a one-step weight loss. These results clearly indicate that the presence of the support decreases the energy change of the decomposed material [3] via the contact surface between the intermediate compounds and the support, which results in the decomposition being favored energetically at the expense of the decomposition of the intermediate compounds. Moreover, it can be suggested that the support, which has a high surface area, may strongly affect the heat change that accompanies the thermal decomposition of the supported solid compound.

(ii) On increasing to 20 mol% AHM, two small endothermic peaks appeared in the DTA curves, while a one-stage weight loss was obtained in the TG curves. These results indicate that the decomposition of AHM on heating up to 400°C occurred in only two steps, instead of three steps as shown for pure AHM.

(iii) On further increasing AHM up to 40 mol%, the decomposition of AHM into MoO_3 took place in three decomposition steps, as for pure AHM. It is worth noting that the presence of γ-alumina during the decomposition of AHM delayed the formation of the first and second intermediates, whereas it favored the decomposition of the second intermediate compound to solid MoO_3.

(iv) The small endothermic peak located at about 100°C is attributed to physically adsorbed water.

(v) The small exothermic peak observed at 417–425°C in the presence of 15 mol% AHM and above, may be due to change in the crystallinity [15] of MoO_3 in the presence of the support.

(vi) The small exothermic peak at about 525°C, which was not accompanied by any weight loss, may be due to the solid–solid interaction between MoO_3 and Al_2O_3 to form a new compound, $Al_2(MoO_4)_3$, as follows

$$3MoO_3 + Al_2O_3 \xrightarrow{>500^\circ C} Al_2(MoO_4)_3 \quad (1)$$

The slight change in peak area accompanying this reaction with increasing AHM may be attributed to the slow rate of formation of aluminum molybdate and also to the small amounts formed.

(vii) The last small endothermic peak centered at about 797°C observed for all mixed samples, and having a peak area that changes little with increased loading may be attributed to the decomposition of $Al_2(MoO_4)_3$ into Al_2O_3 and MoO_3 [10], according to the equation

$$Al_2(MoO_4)_3 \xrightarrow{800^\circ C} Al_2O_3 + MoO_3 \quad (2)$$

The weight loss accompanying this stage corresponds to the sublimation of the resulting MoO_3. It is worth noting that the peak areas accompanying the formation and decomposition of $Al_2(MoO_4)_3$ are similar and little changed for all ratios. This observation may suggest that the formation of aluminum molybdate is similar to its decomposition.

X-ray diffractometry of the thermal products of pure AHM and of AHM supported on γ-alumina

X-ray diffraction lines of the products of pure AHM and of AHM supported on γ-alumina that had been preheated in air at 550, 700 and 900°C for 5 h are shown in Figs. 2–4, respectively. The XRD patterns of AHM supported on γ-alumina in ratios of <20 mol% were first recorded; they were found to be amorphous in nature. This clearly indicates the dispersing effect of the alumina support towards MoO_3 phase; the disappearance of all the diffraction lines of the MoO_3 phase [16, 17] can be attributed to monolayer dispersion of this oxide on the surface of the Al_2O_3 support. Figure 2 shows that the addition of 20, 30 and 40 mol% AHM led to the appearance of lines corresponding to crystallized orthorhombic MoO_3 phase, together with a very small amount of the orthorhombic aluminum molybdate $Al_2(MoO_4)_3$ [10] with diffraction lines located at d(Å) = 3.40 and 4.26. Moreover, the appearance of the diffraction lines of MoO_3 in these samples indicates the limit of the dispersion capacity of Al_2O_3 and MoO_3 solid.

Figure 3 shows the XRD lines of pure MoO_3 and of MoO_3 supported on γ-alumina, derived from different AHM loading ratios, preheated in air at 700°C for 5 h. All the diffraction lines corresponding to MoO_3 phase have disappeared while the diffraction lines corresponding to $Al_2(MoO_4)_3$ have become predominant. This indicates that the molybdenum trioxide present

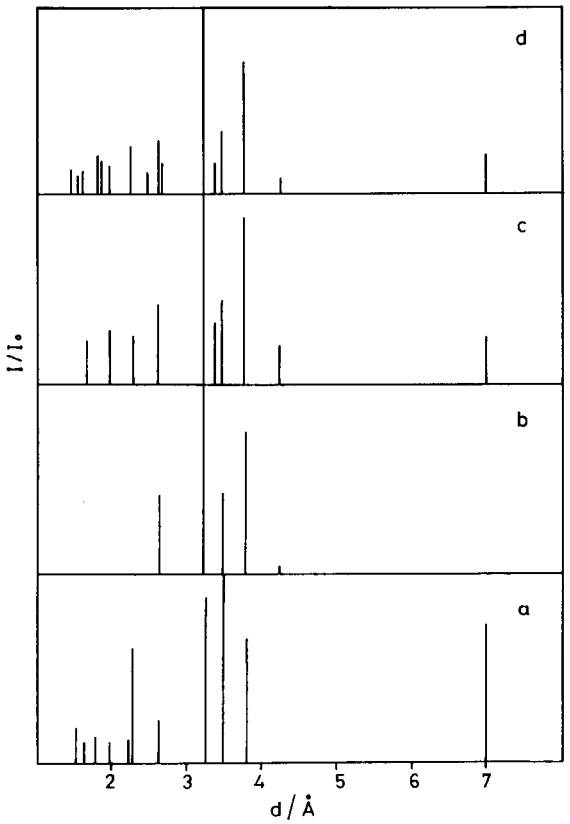

Fig. 2. X-ray diffractograms of the thermal products of pure AHM (a) and of AHM supported on γ-Al_2O_3, loading: 20 mol% (b), 30 mol% (c), and 40 mol% (d). The samples were calcined at 550°C for 5 h.

interacted completely with Al_2O_3 to produce well-crystallized aluminum molybdate phase [10, 12]. The more intensive diffraction lines corresponding to $Al_2(MoO_4)_3$ are located at d(Å) = 3.80 (100), 3.83 (65), 340 (60), 4.02 (47) and 4.27 (37). In addition, it can be observed from Fig. 3 that some lines located at d(Å) = 2.11, 2.58, 2.79, 3.10, 1.85 and 1.64 are obtained. The intensity of these lines is dependent on the ratio of AHM loading. These lines correspond to the crystallized κ-Al_2O_3. However, following the thermal treatment of $Al(OH)_3$ at 500 and 700°C, the XRD patterns indicated that the solid products are amorphous in nature, while the solid calcined at 1000°C consists of crystallized κ-Al_2O_3 together with a small amount of α-Al_2O_3 [18, 19]. Thus, these results indicated that γ-Al_2O_3 can be crystallized at low temperature in the presence of MoO_3, i.e. MoO_3 enhances the crystallization of the treated amorphous γ-alumina.

Figure 4 shows the XRD lines of AHM supported on γ-Al_2O_3 in ratios of 20 and 40 mol% calcined at 900°C for 5 h. The results indicate that all the lines corresponding to $Al_2(MoO_4)_3$ have disappeared, while the lines

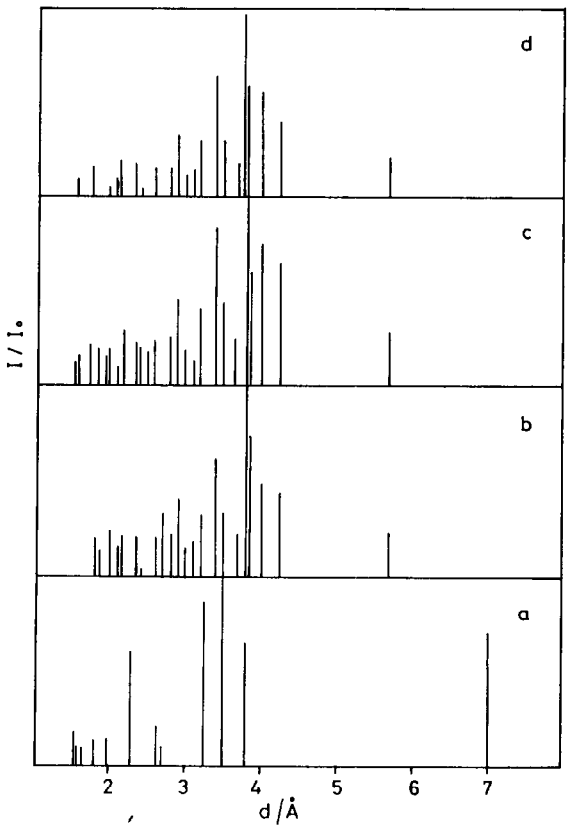

Fig. 3. X-ray diffractograms of the thermal products of pure AHM (a) and of AHM supported on α-Al_2O_3, loading: 20 mol% (b), 30 mol% (c), and 40 mol% (d). The samples were calcined at 700°C for 5 h.

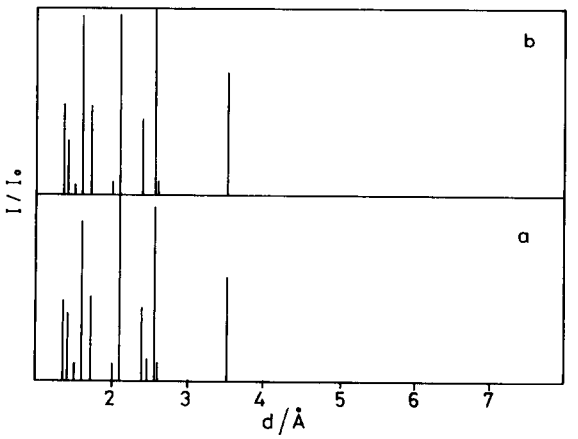

Fig. 4. X-ray diffractograms of the thermal products of AHM supported on γ-Al_2O_3, loading: 20 mol% (a), and 40 mol% (b). The samples were calcined at 900°C for 5 h.

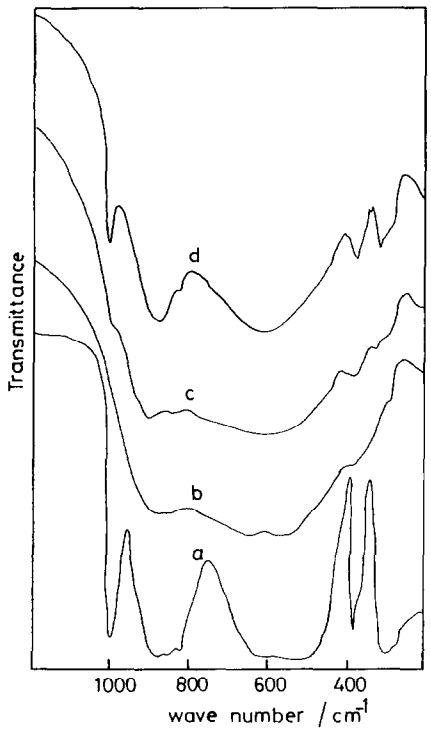

Fig. 5. IR spectra of the thermal products of pure AHM (a) and of AHM supported on γ-Al_2O_3, loading: 20 mol% (b), 30 mol% (c), and 40 mol% (d). The samples were calcined at 400°C for 5 h.

detected correspond to the well-crystallized α-Al_2O_3. The more intensive lines related to α-alumina are located at d(Å) = 2.09, 2.55, 1.60, 3.50, 1.35, 1.40 and 2.40. These results confirm the thermal analysis in which the weight loss obtained above 800°C related to the loss of MoO_3 comes from the decomposition of $Al_2(MoO_4)_3$. Indeed the color of the powder obtained after heating became light to dark grey (α-alumina is white), indicating the formation of MoO_3–Al_2O_3 solid solution. These results suggest that MoO_3 is formed from $Al_2(MoO_4)_3$ and sublimes, partly into a gaseous phase and the remainder dissolves in Al_2O_3 forming a solid solution. It is interesting to mention that the presence of MoO_3 lowers the temperature of crystallinity [18, 19] of α-Al_2O_3 from 1200 to 900°C.

IR spectra of the thermal products of pure AHM and of AHM supported on γ-alumina

The IR spectra of the thermal products AHM and of AHM supported on γ-alumina calcined at 400, 550 and 700°C are shown in Figs. 5–7, respectively. Figure 5, curve a shows that the absorption bands at 990 and

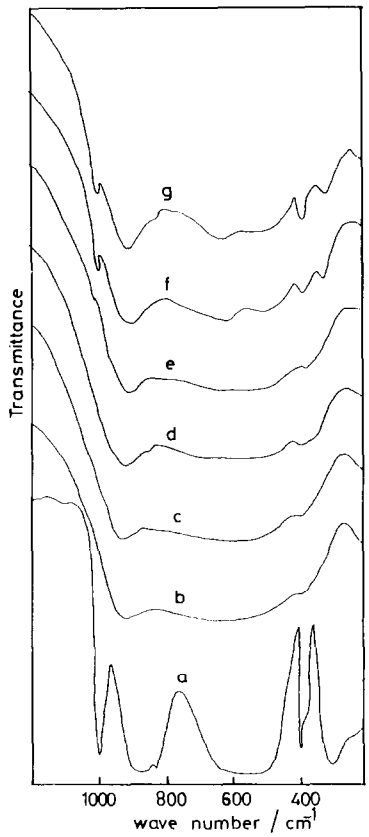

Fig. 6. IR spectra of the thermal products of pure AHM (a) and of AHM supported on γ-Al_2O_3, loading: 15 mol% (b), 20 mol% (c), 25 mol% (d), 30 mol% (e), 35 mol% (f), and 40 mol% (g). The samples were calcined at 550°C for 5 h.

880 cm^{-1} can be attributed to ν(Mo=O) and ν(Mo–O–Mo), respectively [20]. For the supported samples containing AHM up to 20 mol%, the intense absorption of Al_2O_3 (plateau in the 940–520 cm^{-1} region) obscures any diagnostic Mo=O frequency. On increasing the AHM content up to 30 mol%, the two absorption bands corresponding to Mo=O and Mo–O–Mo are only vague, while on further increase up to 40 mol%, the spectrum obtained is similar to that of free MoO_3. These results indicate that the bands corresponding to the surface and bulk frequencies disappear completely with loading of up to 20 mol% AHM. Moreover, none of the bands assigned correspond to the solid–solid interaction between MoO_3 and Al_2O_3.

Figure 6 shows the IR spectra of the thermal products of pure AHM and of AHM supported on γ-alumina calcined at 550°C. A comparison between these spectra and that of pure MoO_3 (curve a) and of that obtained on calcination at 400°C shows the following observations: the absorption

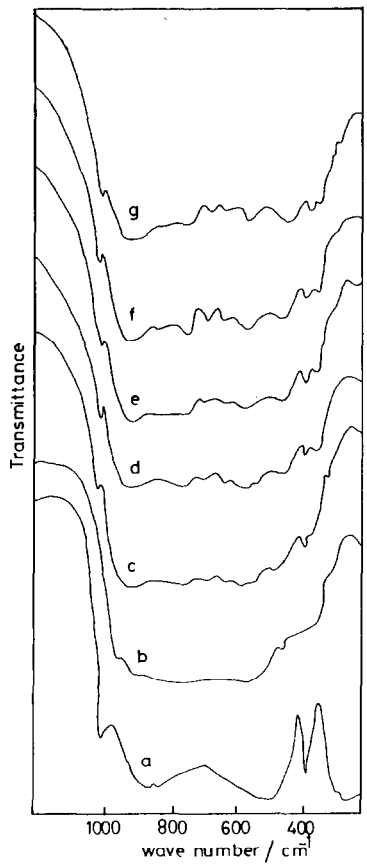

Fig. 7. IR spectra of the thermal products of pure AHM (a) and of AHM supported on γ-Al_2O_3, loading: 15 mol% (b), 20 mol% (c), 25 mol% (d), 30 mol% (e), 35 mol% (f), and 40 mol% (g). The samples were calcined at 700°C for 5 h.

bands corresponding to Mo=O disappeared up to addition of 30 mol% AHM, while they appeared again on further increase to 40 mol%; the band corresponding to the bulk Mo–O–Mo absorption was little affected by the support. The broad band at 900–930 cm^{-1} was attributed to free MoO_3 present in the bulk [21]. In addition, the XRD analysis indicated the formation of a small amount of $Al_2(MoO_4)_3$, while MoO_3 is the most abundant surface phase. Thus, it is interesting to observe that the formation of $Al_2(MoO_4)_3$ on the surface led to the disappearance of only the surface active group, Mo=O.

The IR spectra of the thermal products of pure AHM and of AHM supported on γ-alumina on increasing the calcination temperature to 700°C are shown in Fig. 7. A comparison between these spectra and those shown in Figs. 5 and 6 reveals new absorption bands at 900, 560 and 440 cm^{-1} on addition of 20 mol% AHM. These new bands are attributed to the forma-

tion of aluminum molybdate. Also, the bands characteristic of free MoO_3 were observed. The high purity of the $Al_2(MoO_4)_3$ was confirmed by X-ray analysis and IR spectroscopy [21]. The IR spectra obtained by the KBr disc technique showed characteristic absorption bands at 460 cm^{-1} in accordance with our results. The appearance of the two absorption bands characteristic of MoO_3 on addition of more than 20 mol% suggests the presence of excess MoO_3. However, the XRD results indicated the absence of all characteristic lines corresponding to the MoO_3 crystalline phase. The undetected XRD lines with respect to excess MoO_3 can be explained on the basis that the crystallinity of MoO_3 supported on Al_2O_3 calcined at 700°C is beyond the detection capability of the XRD technique.

CONCLUSIONS

The following main conclusions can be derived from the results obtained.

(i) The thermal decomposition stages of AHM are greatly influenced by the presence of γ-alumina support. The disappearance of all AHM decomposition peaks on the DTA curve on addition of less than 20 mol% AHM results from the dispersion capacity of the alumina surface. However, on increasing the % loading of AHM, γ-Al_2O_3 retards the formation of the first and second intermediate compounds yet enhances the decomposition of the second to produce solid MoO_3.

(ii) MoO_3 readily interacts with Al_2O_3 above 500°C yielding orthorhombic $Al_2(MoO_4)_3$ phase which becomes well crystallized on calcination at 700°C. The aluminum molybdate is thermally stable up to 800°C.

(iii) Heating above 800°C leads to the decomposition of $Al_2(MoO_4)_3$, forming highly crystalline α-Al_2O_3 and MoO_3. The MoO_3 produced is partly volatized and the remaining portion dissolves in the alumina forming MoO_3–Al_2O_3 solid solution.

(iv) Also, the presence of the Al_2O_3 support decreases the crystallinity of MoO_3 while the formation of $Al_2(MoO_4)_3$ only affects the active surface site, Mo=O.

(v) Molybdenum trioxide was found to enhance strongly the crystallization process of κ-Al_2O_3 and α-Al_2O_3 phases at 700 and 900°C respectively.

REFERENCES

1 H.P. Bohem and H. Knözinger, in J.R. Anderson and M. Boudart (Eds.), Catalysis; Science and Technology, Vol. 4, Springer, Berlin, Heidelberg, New York, 1983, p. 39.
2 D.S. Zingg, L.E. Makovsky, R.E. Tischer, F.R. Brown and D.M. Hercules, J. Phys. Chem., 84 (1980) 2898.
3 A.A. Said, J. Mater. Sci., 27 (1992) 5869.
4 A. Maezawa, H. Mitamura, Y. Okamoto and T. Imanata, Bull. Chem. Soc. Jpn., 61 (1988) 2295.

5 Ch. Kordulis, A. Lycourghiots and S. Voliots, Appl. Catal., 15 (1985) 301.
6 R. Lopez, S. Lopez Guerra, J.L.G. Fierro and A. Lopez Agndo, J. Catal., 126 (1990) 8.
7 C.R. Narayanan, S. Srinivasan, A.K. Datye, R. Gorte and A. Biaglow, J. Catal., 138 (1992) 659.
8 D.S. Kim, K. Segawa, T. Soeya and I.E. Wachs, J. Catal., 136 (1992) 539.
9 A.A. Ibrahim and G.A. El-Shobaky, Thermochim. Acta, 147 (1989) 175.
10 J. Leyrer, M.I. Zakai and H. Knözinger, J. Phys. Chem., 90 (1986) 4775.
11 Powder Diffraction File (JCPDS), International Center for Diffraction Data, Swathmore, PA, 1979.
12 A.A. Said and S.A. Halaway, J. Therm. Anal., in press.
13 G.V. Smsonov, The Oxide Hand Book, IFI/Plenum, New York, 1973, pp. 216–7.
14 Hand Book of Chemistry and Physics, Chemical Rubber Publishing Company, Cleveland, OH, 1961, p. 610.
15 A.M. El-Awad, E.A. Hassan, A.A. Said and K.M. Abd El-Salaam, Mh. Chem. für Chemie, 120 (1989) 199.
16 Y.G. Liu, Y.C. Xie, C. Li, Z.Y. Zon and Y.Q. Tang, Cuihua Xuebao, 5 (1984) 234.
17 Y.C. Xie, L.L. Gui, Y.J. Liu, B.Y. Zhao, N.F. Yong, Y.F. Zhang, Q.L. Guo and L.Y. Duan, Proc. 8th Int. Congr. on Catalysis, Huang, 1984, Vol. 5, p. 147.
18 R.C. McKenzie, Seifax Differential Thermal Analysis Data Index, Cleaver-Hume, London, 1962.
19 J.A. Gaden, IR Spectra of Minerals and Related Inorganic Compounds, Butterworths, London, 1975.
20 S.R. Sedonir, S. Abdo and R.F. Howe, J. Phys. Chem. Lett., 86 (1982) 233.
21 N. Giordano, J.C.J. Bart, A. Vaghi, A. Castellan and G. Matinotti, J. Catal., 36 (1975) 81.